Hydrology Research

Hydrology Research Vol 55 No 2, 144 doi: 10.2166/nh.2023.181

Boosting hydropower generation of mixed reservoirs for reducing carbon emissions by using a simulation–optimization framework

Yanfeng He[a,b,c], Shenglian Guo[a], Yanlai Zhou[a,*], Di Zhu[a], Hua Chen[a], Lihua Xiong[a], Jie Liu[a,d] and Chong-Yu Xu[e]

[a] State Key Laboratory of Water Resources Engineering and Management, Wuhan University, Wuhan 430072, China
[b] Power China Chengdu Engineering Corporation Limited, Chengdu 610072, China
[c] Technological Innovation Center of Hydropower, Wind, Solar and Energy Storage of Tibet Autonomous Region, Chengdu 610072, China
[d] School of Architecture and Civil Engineering, Chengdu University, Chengdu 610106, China
[e] Department of Geosciences, University of Oslo, P.O. Box 1047 Blindern, Oslo N-0316, Norway
*Corresponding author. E-mail: yanlai.zhou@whu.edu.cn

YZ, 0000-0002-5447-2420

ABSTRACT

The optimization operation of reservoir seasonal Flood-Limited Water Levels (FLWLs) can counterbalance the hydropower generation and flood prevention in the flood season. This study proposes a multi-objective optimization operation model to optimize the reservoir seasonal FLWLs for enhancing synergies of hydropower generation and flood prevention. The integration of the Non-dominated Sorting Genetic Algorithm-II and a simulation-optimization framework is applied for optimizing the joint operation of reservoirs meanwhile achieving the Pareto solutions to reduce computation complexity and time. And then, the Technique for Order of Preference by Similarity to Ideal Solution is utilized to identify the best seasonal FLWL scheme grounded on multi-criteria decision-making analysis. The mixed reservoirs located in the upstream Yangtze River of China constitute the case study. The results showed that: compared with the annual FLWL scheme, the proposed seasonal FLWL schemes without increasing flood prevention risk could facilitate the joint operation of the mixed reservoirs to achieve 868 million kW·h (5.1% improvement) in average hydroelectricity production during the flood season, meanwhile reducing 681 million kg in carbon emissions accordingly. The results support that the proposed methods can boost hydropower production to benefit China's national tactics in accomplishing peak carbon dioxide emissions before 2030.

Key words: hydropower sustainability, multi-objective optimization, non-dominated sorting genetic algorithm-II, reservoir operation, Yangtze River

HIGHLIGHTS

- This study aimed to optimize the joint operation of reservoirs to promote sustainable energy development.
- This study also aimed to improve hydropower output and flood prevention meanwhile reducing CO_2 emissions.
- The NSGA-II and simulation–optimization structure were integrated to attain Pareto solutions.
- Intelligent decision-making facilitates new energy and floodwater management.

GRAPHICAL ABSTRACT

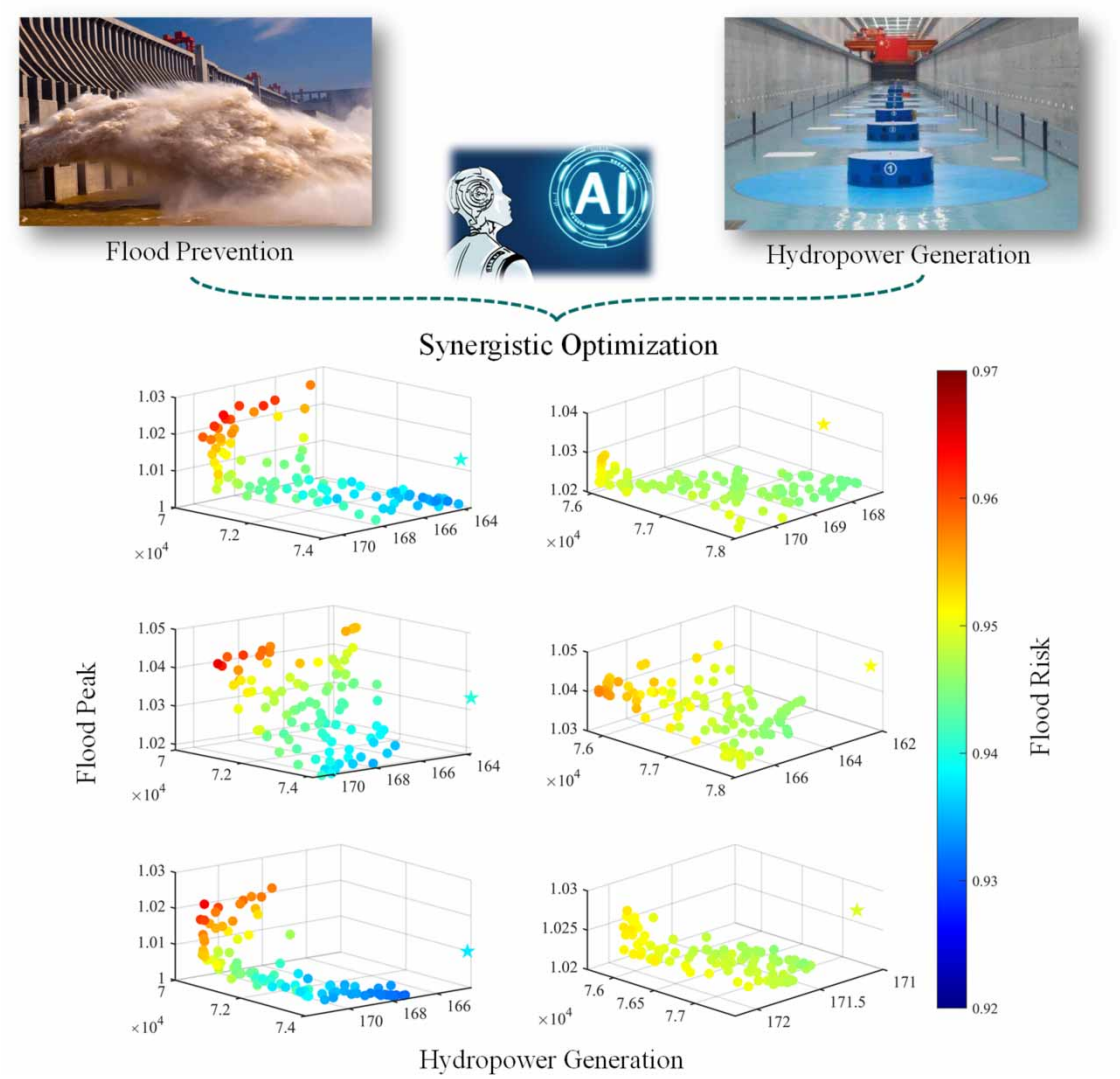

1. INTRODUCTION

Reservoir joint operation is an important and efficient non-engineering measure for promoting renewable energy production, water resources management and carbon emissions reduction (Berga 2016; Kuriqi *et al.* 2019; Tamm & Tamm 2020; Wegner *et al.* 2020; Spanoudaki *et al.* 2022). As one of the important parameters of reservoir operation, the flood-limited water level (FLWL) is usually used to make a tradeoff between flood prevention and hydropower production (Zhou *et al.* 2014; Liu *et al.* 2015a, 2015b; Zhu *et al.* 2022a, 2022b, 2022c). The standard operation policy (SOP) of annual FLWL, in general, can allow ample storage capacity for flood prevention; however, it often gives rise to large spilled water and low impoundment water volume in the flood season (Li *et al.* 2014; Yazdi & Moridi 2018; Liu *et al.* 2022). Considering flood seasonality, the optimization of seasonal FLWLs is beneficial to largely facilitate the development and utilization of flood resources without lowering flood prevention standards, compared with the SOP of annual FLWL.

The optimal operation of FLWLs of reservoirs is a vital approach for satisfactorily balancing flood prevention and hydroelectricity needs (Yun & Singh 2008; Chen *et al.* 2017). In general, under the same hydrological conditions, the larger the value of the FLWL is set to be, the higher the reservoir flood risk will be. In contrast, the benefits of floodwater resources utilization such as hydropower generation (HG) and water supply will be decreased largely if the value of the FLWL is set to be low. Given the benefits and cost of hydraulic infrastructures, the annual FLWL is calculated by flood regulation

simulation based on the annual maximum design floods corresponding to some critical return periods (Li *et al.* 2010). Since annual maximum design floods do not consider flood seasonality, a reservoir will adopt a small and single value of the annual FLWL resulting in a low floodwater resources utilization efficiency (Xiong *et al.* 2020). Hence, it is desired to conduct more intensive research on the optimization of seasonal FLWLs in consideration of the flood seasonality to boost hydropower output and floodwater utilization efficiency of reservoirs.

Recently, several studies have been conducted to improve floodwater operation and management without updating hydraulic infrastructures, from the perspectives of flood season segmentation and seasonal FLWL operation (Jiang *et al.* 2019; He *et al.* 2022). The flood season segmentation often divides the whole flood season into two or three sub-season segments, and then each sub-season will set an FLWL accordingly. For instance, genesis analysis (Singh *et al.* 2005), fractal theory (Fang *et al.* 2010), change-point analysis (Liu *et al.* 2010), the statistical method (Dhakal *et al.* 2015), entropy-based method (Singh 2011), fuzzy set analysis (Mu *et al.* 2022), and so on, have been applied for analyzing the flood seasonality to accomplish the season segmentation. Following up flood season segmentation, some researchers focus on determining seasonal FLWL operation schemes from the standpoint of risk–benefit analysis. The risk analysis model proposed by Zhou *et al.* (2015) can adequately assess the impact of the uncertainties consisting of hydrology input, water release capacity and reservoir storage capacity on the values of seasonal FLWLs by using the Monte Carlo simulation method. In comparison to the SOP of annual FLWL, Liu *et al.* (2015a, 2015b) constructed an optimization operation model to identify the seasonal FLWL scheme of the Three Gorges Reservoir (TGR) for three sub-season segments without increasing the reservoir flood prevention risk. In addition, the joint optimization operation of reservoirs and their floodplains is also an efficient approach for increasing the values of seasonal FLWLs to stimulate the comprehensive benefits of hydropower and floodwater resources (Xie *et al.* 2018). Kim *et al.* (2022) introduced a resilience framework to optimize reservoir hydropower operation for mitigating the power loss due to seasonal FLWL control. Wan *et al.* (2023) proposed a multi-objective synergistic decision-making method to optimize the FLWL scheme of the Xianghongdian Reservoir for making tradeoffs between HG benefits and flood prevention risk. The existing studies have been focusing on optimizing the seasonal FLWL schemes for single reservoir operation, whereas none of the studies have been carried out to optimize season FLWL schemes for mixed reservoirs. As known, with an increasing number of reservoirs, it is highly complex and challenging for researchers to model and optimize the seasonal FLWL management system, because more complicated hydraulic connections and more constraints and decision variables need to be considered in the model (Giuliani *et al.* 2021). Thus, it is crucial to explore the seasonal FLWL management system of mixed reservoirs for facilitating hydropower production expansion while stimulating floodwater resources utilization benefits.

The innovative nature of this study is indebted to optimizing HG and flood prevention operation using an evolutionary algorithm with the simulation–optimization framework, and its application is, for the first time, to promote the new niche of floodwater utilization. The new contribution of this study is threefold: proposing a multi-objective optimization operation model of seasonal FLWLs of mixed reservoirs; integrating the NSGA-II and a simulation–optimization framework to reduce computation complexity and time caused by plenty of variables and constraints related to modeling the seasonal FLWL management system of mixed reservoirs; and utilizing the technique for order of preference by similarity to ideal solution (TOPSIS) to identify the best operation scheme of seasonal FLWLs from the perspective of multi-criteria decision-making analysis. The proposed approach is applied to a mixed reservoir system composed of the TGR and six other reservoirs located in the upstream Yangtze River of China.

2. STUDY AREA AND DATA

As the longest river in China, the Yangtze River has a 6,397 km length with a 1.8 million km^2 drainage area. In the Yangtze River basin, over 50,000 reservoirs have been constructed to satisfy the needs of flood prevention and water resource development. Among them, the TGR, with 22,500 MW of installed power capacity and 393×10^8 m^3 of total storage capacity, is the largest dam and hydroelectric project ever built in the world to date (Zheng *et al.* 2016). The Dongting Lake is the second largest freshwater lake in China and is situated in the middle Yangtze River (Figure 1(a)). Its surface water area would usually change between 710 km^2 (dry season) and 2,690 km^2 (flood season) (Gao *et al.* 2017). Six reservoirs named as Jiangya (JY), Zaoshi (ZS), Fengtan (FT), Wuqiangxi (WQX), Dongjiang (DJ) and Zhexi (ZX), have been constructed in the four tributaries of the Dongting Lake basin for the purposes of HG and flood protection of the Chenglingji flood prevention station by joint operation with the TGR (Figure 1(b)). Table 1 summarizes the key parameters of the seven reservoirs.

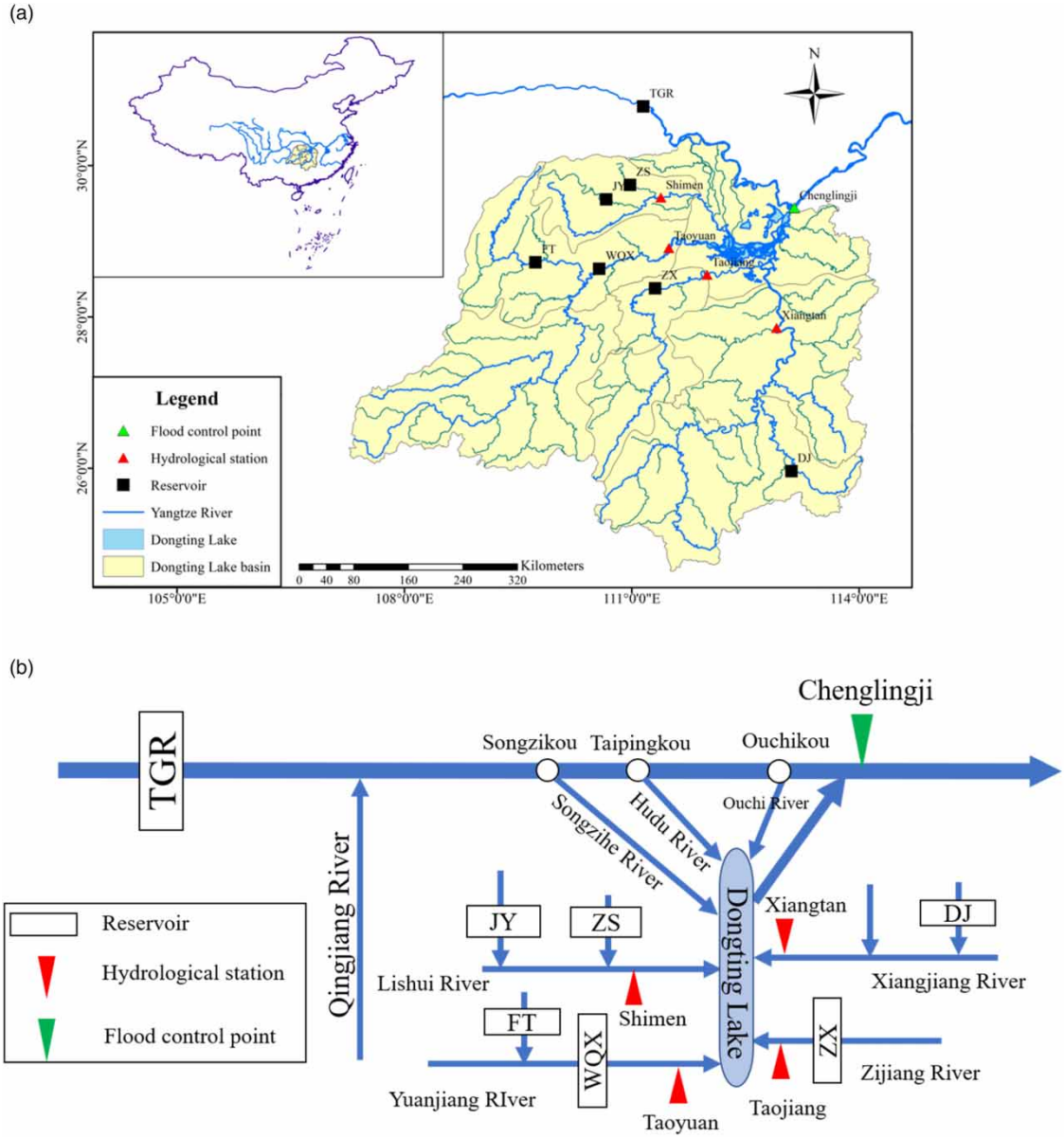

Figure 1 | The generalized diagram of the mixed reservoirs in the Yangtze River and Dongting Lake.

Table 1 | The key parameters of the seven reservoirs

Name	Basin area (in 1,000 km^2)	Flood control capacity (10^8 m^3)	Annual FLWL (m)	Flood high WL (m)	Install capacity (MW)
TGR	1,000.0	221.50	145.0	175.0	22,500
JY	3.7	7.40	210.6	236.0	300
ZS	3.0	7.83	125.0	143.5	120
FT	17.5	2.77	198.5	205.0	815
WQX	83.8	13.60	98.0	108.0	1,200
DJ	4.7	7.46	284.0	288.6	500
ZX	22.6	10.60	162.0	170.0	1,050

Seven representative flood events, including 1956 and 2007 (first sub-season segment); 1954, 1981, and 1998 (second sub-season segment); and 1952 and 1964 (third sub-season segment), were utilized for calculating the design flood hydrographs corresponding to 5, 1 and 0.1% occurrence frequencies in accordance with the flood peak–flood volume magnification method (Xiao *et al.* 2009; Zhou *et al.* 2015). The design flood hydrographs of the TGR are taken as an example, which are displayed in Figure A1. The durations of the flood event are 30, 30 and 15 days in the first, second and third sub-season segments, respectively. The calculation time step is 1 day in each flood event. These data have been calibrated and provided by the Bureau of Hydrology, Changjiang Water Resources Commission. The lower and upper boundaries of seasonal FLWLs of the mixed reservoirs in the three sub-season segments are listed in Table 2. The lower boundaries of seasonal FLWLs are equal to the annual FLWLs of the reservoirs and the upper ones are referred to the previous study (Liu *et al.* 2015a, 2015b).

3. METHODS

The architecture of the seasonal FLWL management system proposed here is displayed in Figure 2, containing three pivotal parts. The operation model of seasonal FLWLs was first constructed with four objectives and physical constraints to increase the hydropower output (O1) and meet the three requirements (O1, O2 and O3) of flood prevention simultaneously (Figure 2(a)). Then, the model of the seasonal FLWLs was optimized using the simulation–optimization framework (Figure 2(b)) driven by various representative flood events at a 1-day scale. Finally, the best seasonal FLWL scheme was identified by multi-criteria decision-making analysis (Figure 2(c)). The description of the used methods is presented below.

3.1. Multi-objective operation model of seasonal FLWLs

The multi-objective operation model is constructed to tackle seasonal FLWL management challenges by increasing hydroelectricity output while guaranteeing flood prevention safety.

3.1.1. Objective functions

In the flood season, the model (Figure 2(a)) is constructed to simultaneously accomplish four objectives for synergistically maximizing HG and alleviating flood prevention pressure, which are Objective 1: maximization of the HG of reservoirs; Objective 2: minimization of the peak streamflow (PF) of the flood control station, which is suitable for operating small–medium (occurrence frequency $\leq$5%) flood events; Objective 3: minimization of the final water level (WL) of the reservoir at the flood prevention period, which is suitable for operating large (1% $<$ occurrence frequency $\leq$ 5%) flood events; Objective 4: minimization of the highest reservoir WL (HWL), which is suitable for operating extra-large (occurrence frequency $\leq$1%) flood events.

O1: maximize HG,

$$\mathrm{O1} = \max \mathrm{HG} = \max \sum_{i=1}^{I} \sum_{t=1}^{T} P_i(t) \cdot \Delta t \tag{1}$$

Table 2 | The lower and upper boundaries of seasonal FLWLs of the mixed reservoirs in the three sub-season segments

Reservoir	Lower boundary of FLWL = annual FLWL (m)	Upper boundary of seasonal FLWL (m)		
		First sub-season segment (pre-flood season)	Second sub-season segment (main-flood season)	Third sub-season segment (post-flood season)
TGR	145.0	155.0	150.0	154.0
JY	210.6	218.6	215.6	217.6
ZS	125.0	133.0	130.0	132.0
FT	198.5	201.5	200.5	201.5
WQX	98.0	102.0	100.0	103.0
DJ	284.0	286.0	285.0	286.0
ZX	162.0	165.0	164.0	165.0

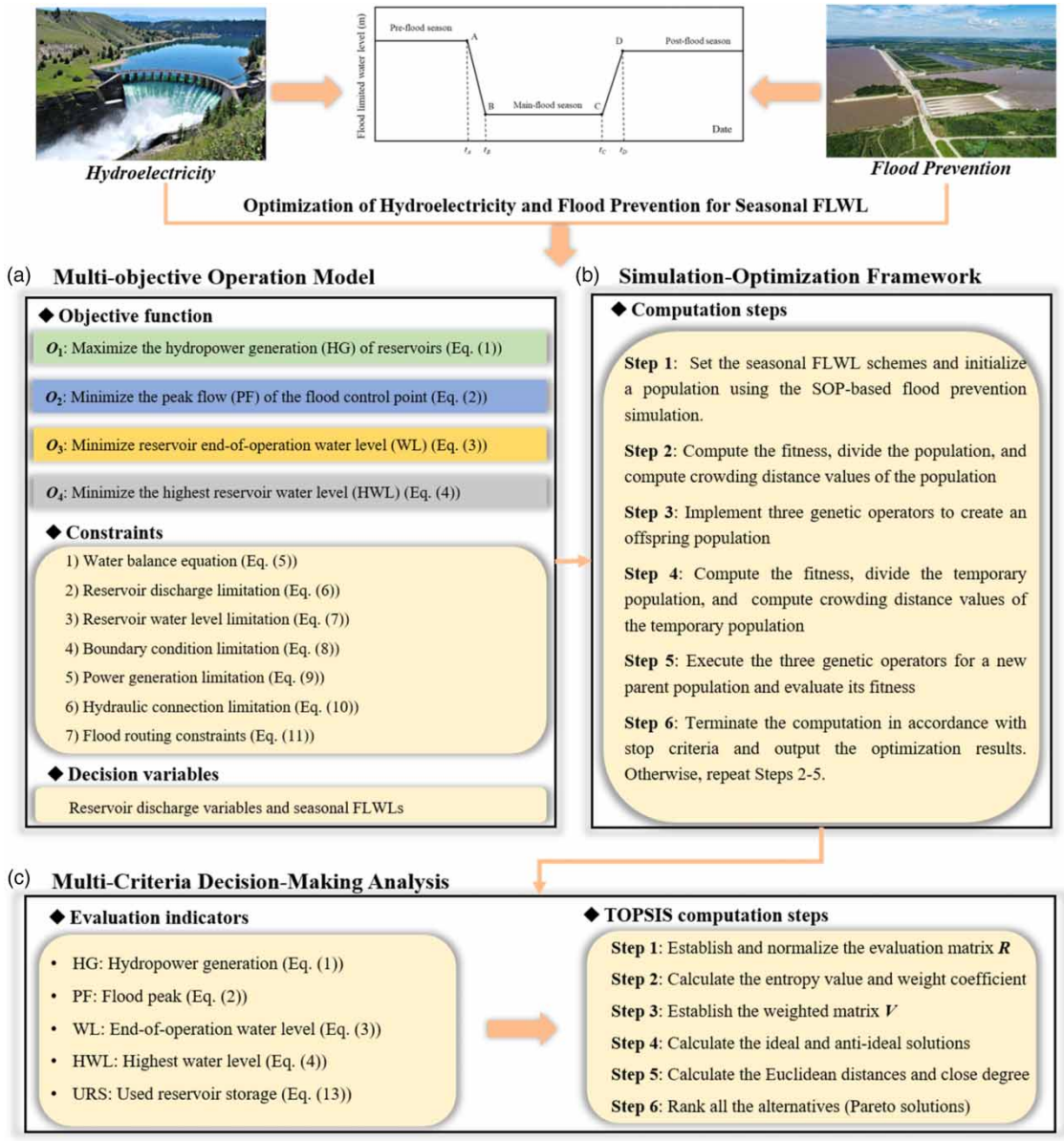

Figure 2 | The architecture of the seasonal FLWL management system. (a) Multi-objective operation model. (b) Simulation–optimization framework. (c). Multi-criteria decision-making analysis.

O2: minimize PF,

$$\mathrm{O2} = \min \mathrm{PF} = \min\{\max[Q(1), Q(2), \ldots, Q(t), \ldots, Q(T)]\} \tag{2}$$

O3: minimize WL,

$$\mathrm{O3} = \min \mathrm{WL} = \min\left\{\frac{\sum_{i=1}^{I} Z_i(T+1)/Z_i^{\mathrm{end}}}{I}\right\} \tag{3}$$

O4: minimize *HWL*,

$$\mathrm{O4} = \min \mathrm{HWL} = \min \left\{ \frac{\sum_{i=1}^{I} \max\left[Z_1(1),\ \ldots,\ Z_i(t),\ \ldots Z_i(T+1)\right]/Z_i^{\max}}{I} \right\} \tag{4}$$

where $Q(t)$ is the streamflow of the flood control station at time t, $Z_i(t)$ is the WL of the ith reservoir at the tth time, $P_i(t)$ is the power generation of the ith hydropower plant at the tth time, Δt is the calculation time interval, Z_i^{end} is the targeted WL of the ith reservoir at the flood prevention period and T and I are the numbers of regulating periods and reservoirs, respectively.

3.1.2. Constraints

The physical constraints are listed below:

(1) Reservoir water balance equation:

$$[q_i^{\mathrm{in}}(t) - q_i^{\mathrm{out}}(t)] \cdot \Delta t = V_i(t+1) - V_i(t) \tag{5}$$

where $q_i^{\mathrm{in}}(t)$ and $q_i^{\mathrm{out}}(t)$ are the inflow and water release (i.e., discharge) of the ith reservoir at the tth time, respectively.

(2) Reservoir discharge limitation:

$$q_i^{\mathrm{out}}(t) \le f[Z_i(t)] \tag{6a}$$

$$q_i^{\mathrm{out}}(t) \le \min\left(q_i^{\mathrm{in}}(t), f[Z_i(t)]\right)(t \le T_i^{\mathrm{peak}}) \tag{6b}$$

where $f[\cdot]$ represents the maximum reservoir water release corresponding to the reservoir WL and T_i^{peak} is the occurrence time of the maximal inflow (i.e., flood peak) of the ith reservoir in the flood event.

(3) Reservoir WL limitation:

$$\mathrm{ZL}_i(t) \le Z_i(t) \le \mathrm{ZU}_i(t) \tag{7}$$

where $ZL_i(t)$ and $ZU_i(t)$ are the minimal and maximal WLs of the ith reservoir at the tth time, respectively.

(4) Initial WL limitation:

$$Z_i(1) = \mathrm{Z}_i^{\mathrm{seasonal}} \tag{8}$$

where $\mathrm{Z}_i^{\mathrm{seasonal}}$ is the seasonal FLWL (=initial WL) of the ith reservoir.

(5) Power generation limitation:

$$PL_i(t) \le P_i(t) \le PU_i(t) \tag{9}$$

where $PL_i(t)$ and $PU_i(t)$ are the minimum and maximum power generation of the ith reservoir at the tth time, respectively.

(6) Hydraulic connection limitation:

$$q_i^{\mathrm{in}}(t) = q_{i-1}^{\mathrm{out}}(t) + \Delta q_i(t) \tag{10}$$

where $\Delta q_i(t)$ is the lateral flow in the upstream of the ith reservoir at the tth time.

(7) Flood routing constraint:

The flood routing of the Dongting lake basin is calculated by the channel storage equation of the lake (Sun *et al.* 2020).

$$S(t) = g(Q(t), I(t), Z_{\mathrm{Luo}}(t)) \tag{11a}$$

$$\left[\frac{I(t)+I(t+1)}{2}-\frac{Q(t)+Q(t+1)}{2}\right]\Delta t = S(t+1)-S(t) \tag{11b}$$

where $I(t)$ is the total inflow of the Dongting lake at the tth time, $S(t)$ is the channel storage at the tth time, $g(*)$ is the channel storage curve, and $Z_{\mathrm{Luo}}(t)$ is the WL of the Luoshan station (i.e., the outlet of the Dongting lake basin) at the tth time.

3.2. Simulation–optimization framework

The SOP-based (Figure 3) flood prevention simulation is commonly utilized to calculate the values of seasonal FLWLs (Zhou *et al.* 2014, 2015; Ma *et al.* 2020), where the seasonal FLWL is used as the initial WL (see Equation (8)) to regulate flood events. The SOP-based flood prevention simulation has good applicability due to the merit of operational simplicity. Although the SOP has succeeded in coping with a variety of reservoir operation and renewable energy management (Zhou *et al.* 2019, 2020), it, similar to other non-optimization algorithms, cannot search for the optimal flood prevention solution; this is especially true in the complex multi-objective and joint operation of the mixed reservoirs. In addition, the operation model of the seasonal FLWL management system is intrinsically a complex non-convex mathematical problem associated with plenty of physical constraints, where the non-differentiable and non-linear equations induce the model to encounter several local minima phenomena. To be specific, the HG (Equation (1)) objective function and three flood prevention objective functions (Equations (2)–(4)) are used to tackle three kinds (small–medium, large, extra-large) of flood magnitude events, while the physical constraints are related to the dynamic hydraulic connections and the static reservoir characteristics. Despite the fact that the NSGA-II (Deb *et al.* 2000) can be successful in searching a wide set of Pareto solutions, it has a technical bottleneck for tackling the non-differentiable and non-linear mathematical problems, due to the dimensionality curse. Since the amount of physical constraints and reservoir discharges (i.e., decision variables) is enormous and they have both close interactions and intrinsic influences, finding the optimization solution to the non-differentiable and non-linear multi-objective operation model has become a big challenge.

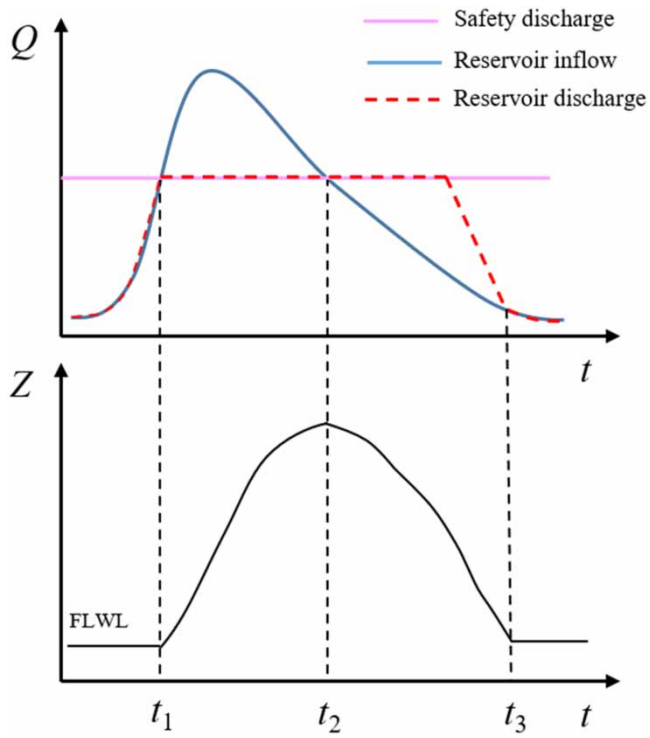

Figure 3 | The feasible operation policies using the SOP-based flood prevention simulation.

Owing to the fast development of cloud computing, such complex mathematical problems can be handled with less computation time and much more efficiency. As known, the NSGA-II optimization algorithm has the ability to combine simulation methods to tackle the multi-objective optimization operation model (Zhang *et al.* 2019; Gonzalez *et al.* 2020; Hatamkhani *et al.* 2020). Hence, this study fused the SOP-based flood prevention simulation into the standard NSGA-II optimization algorithm to boost the performance of the multi-objective and joint operation model of seasonal FLWLs (i.e., the simulation–optimization framework). Because the intelligent optimization algorithm cannot ensure that the initial population includes feasible operation policies, the NSGA-II would be easy to fall into the local minima. For the proposed simulation–optimization framework, feasible operation policies for reservoir flood prevention are first created by the SOP-based flood prevention simulation, and then the optimal solution is searched efficiently by integrating the feasible operation policies into the initial population of the NSGA-II. In other words, fusion of feasible operation policies into the NSGA-II can effectively facilitate the search for Pareto Frontier with far less computation time, and thus could increase the capability of escaping from local optimum to find global optimum. The simulation (SOP)–optimization (NSGA-II) structure executes the below calculation steps.

Step 1: Set the seasonal FLWL schemes and initialize a population N_0 of size NP using the SOP-based flood prevention simulation (Figure 3) for each reservoir. In Figure 3, before the time t_1 of raising WL, if the inflow is smaller than the reservoir water release capacity (see Equation (6b)), the reservoir water release is set to be the inflow, and thus the WL would maintain the seasonal FLWL. From the time t_1 up to the time t_2 (t_2 is the occurrence of the HWL), the inflow increases gradually to be larger than the water release capacity, then the reservoir would implement water release in accordance with the water release capacity as well as the WL would reach the maximum value at the time t_2 (reservoir discharge = reservoir inflow). After the time t_2, the WL decreases with the decline in reservoir inflow gradually.

Step 2: Compute the fitness values of the N_0; divide the initial population N_0 into various ranks by using the non-dominated sorting method; and then compute crowding distance values of the initial population N_0.

Step 3: Produce the offspring population corresponding to the next generation by using the hybrid of the crowded tournament selection operator and the elitism preservation strategy; integrate parent chromosomes to create a new offspring one by using the crossover operator with a probability of p_1; and increase genetic diversity of the population by using the mutation operator with a probability of p_2. Therefore, an offspring population A_0 of size NP would be constructed with the three genetic operators.

Step 4: For each generation j, calculate the fitness values of A_j; integrate A_{j-1} and A_j into a temporary population B_j of size $2 \times$ NP; divide the temporary population B_j into various ranks; and compute the crowding distance values of the temporary population B_j.

Step 5: Execute the crowed tournament selection operator to choose an N_{j+1} of size NP from N_j; implement genetic operators to create an A_{j+1} of size NP; and calculate the fitness values of N_{j+1} and A_{j+1}.

Step 6: Repeat Steps 2–5 to decide whether the calculation would be terminated according to the stop criteria. When the number of iterations is smaller than the maximum iteration (K), then Steps 2–5 would be repeated. Otherwise, output the optimal solutions associated with decision variables.

In our case, the multi-objective operation model would be driven by a number of 3,780 datasets (=7 reservoirs $\times$ 45 days (first and third sub-season segments) $\times$ 2 representative flood events $\times$ 3 return periods + 7 reservoirs $\times$ 30 days (second sub-season segment) $\times$ 3 representative flood events $\times$ 3 return periods, consisting of 3,780 decision variables (i.e., water release variables) and 15,120 physical constraints (=4 equations $\times$ 3,780 water release variables). After executing the SOP-based flood prevention simulation, plenty of initial solutions would be provided to meet the requirements of 15,120 physical constraints, which means the capability of the NSGA-II for searching global optimum would be largely raised. The parameters of the used NSGA-II for achieving the Pareto frontier were set as NP = 100, $K = 500$, $p_1 = 0.8$ and $p_2 = 0.1$.

3.3. TOPSIS-based multi-criteria decision-making analysis

Some multi-criteria decision-making methods were employed to identify the best scheme among a large amount of alternatives (Sánchez-Lozano *et al.* 2016; Tamimi *et al.* 2021; Zhu *et al.* 2022a, 2022b, 2022c). Because the TOPSIS has the ability to offer an opportunity for stakeholders and decision-makers on assessing and pre-experiencing the consequences of various best solutions, it was adopted to identify the best operation scheme from the Pareto solutions (i.e., alternatives) by considering flood prevention safety and HG benefits. The calculation steps of the TOPSIS-based multi-criteria decision-making analysis are described below.

Step 1: Establish the evaluation matrix $\boldsymbol{R}$ with normalization.

$$\boldsymbol{R} = (r_{i,j})_{m\times n} = \begin{Bmatrix} r_{1,1} & \cdots & r_{1,n} \\ \vdots & \ldots & \vdots \\ r_{m,1} & \cdots & r_{m,n} \end{Bmatrix} \tag{12}$$

where $r_{i,j}$ is the jth indicator of the ith alternative. m and n are the numbers of alternatives and indicators, respectively. In our case, five indicators consisting of the HG (Equation (1)), the PF (Equation (2)), the WL (Equation (3)), the HWL (Equation (4)) and the used reservoir storage for flood prevention (URS) are adopted to construct the evaluation matrix. The computation equation of the URS is described as follows:.

$$\text{URS} = \sum_{i-1}^{\text{I}} \{f_i^{\text{zv}}(\max[Z_1(1), \ldots, Z_i(\text{t}), \ldots Z_i(T+1)]) - f_i^{\text{zv}}(Z_i(1))\} \tag{13}$$

where $f_i^{\text{zv}}(\cdot)$ is the curve of reservoir storage capacity corresponding to the WL in the ith reservoir.

$$y_{i,j} = \begin{cases} \dfrac{r_{i,j} - r_j^{\min}}{r_j^{\max} - r_j^{\min}} & \text{if } r_{i,j} \text{ is the benefit indicator} \\ \dfrac{r_j^{\max} - r_{i,j}}{r_j^{\max} - r_j^{\min}} & \text{if } r_{i,j} \text{ is the cost indicator} \end{cases} \tag{14}$$

where $y_{i,j}$ is the normalized value of $r_{i,j}$ and $r_j^{\max}$ and $r_j^{\min}$ are the maximum and minimum of the jth indicator.

Step 2: Calculate the entropy values of the indicators and their weight coefficients.

$$e_j = -\frac{1}{\ln m}\sum_{i=1}^{m} f_{i,j}\ln(f_{ij}) \tag{15}$$

$$f_{ij} = \frac{y_{i,j}}{\sum_{i=1}^{m} y_{i,j}} \tag{16}$$

where e_j is the entropy value of the jth indicator.

$$W_j = \frac{1-e_j}{\sum_{j=1}^{n}(1-e_j)} \tag{17}$$

where W_j is the entropy weight of the jth indicator.

Step 3: Establish the matrix $\boldsymbol{V}$ of entropy weights.

$$\boldsymbol{V} = (v_{i,j})_{m\times n} = \begin{Bmatrix} v_{1,1} & \cdots & v_{1,n} \\ \vdots & \ldots & \vdots \\ v_{m,1} & \cdots & v_{m,n} \end{Bmatrix} \tag{18a}$$

$$v_{i,j} = W_j y_{i,j} \tag{18b}$$

Step 4: Compute the ideal and anti-ideal operation solutions of seasonal FLWLs.

$$\begin{cases} \boldsymbol{A}^+ = \{v_1^+, \ldots v_j^+, \ldots, v_n^+\} \\ \boldsymbol{A}^- = \{v_1^-, \ldots v_j^-, \ldots, v_n^-\} \end{cases} \tag{19}$$

where $\boldsymbol{A}^+$ and $\boldsymbol{A}^-$ are the ideal and anti-ideal operation solutions of seasonal FLWLs. $v_j{}^+$ and $v_j{}^-$ can be calculated as follows:

$$\begin{cases} v_j^+ = \max\{v_{i_j}, i = 1, \ldots, m\} \\ v_j^- = \min\{v_{i_j}, i = 1, \ldots, m\} \end{cases} \text{for the benefit} - \text{type indicator} \tag{20a}$$

$$\begin{cases} v_j^+ = \min\{v_{i,j}, i = 1, \ldots, m\} \\ v_j^- = \max\{v_{i_j}, i = 1, \ldots, m\} \end{cases} \text{for the cost} - \text{type indicator} \tag{20b}$$

Step 5: Compute the Euclidean distance between each alternative and the ideal (or anti-ideal) solution and calculate the close degree C_i.

$$\begin{cases} D_i^+ = \sqrt{\sum_{j=1}^{n} (v_{i,j} - v_j^+)^2} \\ D_i^- = \sqrt{\sum_{j=1}^{n} (v_{i,j} - v_j^-)^2} \end{cases} \tag{21}$$

The larger C_i reflects more proximity between the ith alternative and the ideal solution, which can be calculated as follows:

$$C_i = \frac{D_i^-}{D_i^- + D_i^+} \tag{22}$$

Step 6: Rank all the alternatives (i.e., Pareto solutions) in accordance with the value of the close degree and select the best operation solution of seasonal FLWLs corresponding to the largest close degree.

4. RESULTS AND DISCUSSION

4.1. Hydroelectricity output (O1) and flood prevention (O2–O4) optimization by the NSGA-II

The Pareto frontiers of HG (O1: HG) versus flood prevention operation (O2: PF, O3: WL, O4: HWL) from the NSGA-II corresponding to the first, second, and third sub-season segments are presented in Figures A2, 4(a -i) and A3, respectively. It is noted that the position of the SOP solution is far away from the Pareto frontiers of HG and flood prevention operation. The indicator values of the O1 (O2) of the Pareto solutions are larger (smaller) than those of the SOP solution. Taking the design flood with the 20-year return period based on the 1956 representative flood event (shown in FigureA2(a)), for example, the HG (O1: HG) and peak flow (O2: PF) of the Chenglingji flood control point using the SOP solution are 122×10^8 kW h and 50,658 m^3/s, respectively, while the HG (O1: HG) of the Pareto solutions ranges from 127 to 135×10^8 kW h with smaller values of the O2 ($\leq$50,000 m^3/s). In addition, the values of the O1 raise with the decline in the O2 and the increase of the O3 and the O4.

For the first sub-season segment (Figure A2), the values of the HWL (O4) obtained from the Pareto solutions are larger than those of the SOP solution. Due to the increasing magnitude of design floods, the range of hydropower outputs from the Pareto solutions increases from 128–131 $\times 10^8$ kW h (Figure A2(e)) to 151–153 $\times 10^8$ kW h (Figure A2(c)) accordingly. For the second sub-season segment, especially for the design floods with the 1,000-year return period (Figure 4(c), 4(f) and 4(i)), there are dozens of Pareto solutions where the values of the four objectives (O1–O4) are better than those of the SOP solution, indicating that the Pareto solutions can optimize the hydroelectricity production and the flood prevention operation simultaneously. For the third sub-season segment (Figure A3), considering the shorter flood prevention operation period (15 days), the HG of the Pareto-front solutions is less than that of the Pareto-front solutions concerning the first sub-season segment (30 days) and the third sub-season segment (30 days) correspondingly. Due to the similar flood magnitudes, the distribution of the Pareto solutions in the first sub-season segment is similar to that of the Pareto solutions in the third sub-season segment.

There is a synergistic relationship between HG (O1) and the PF of the flood control station (O2), while the final WL of the reservoir at the flood prevention period (O3) and the HWL (O4) are competitive with the O1 and the O2. Overall, the Pareto solutions of the NSGA-II have the ability to counterbalance hydroelectricity production and flood prevention operation simultaneously to respond to various magnitudes (i.e., small–medium, large, and extra-large) of flood events.

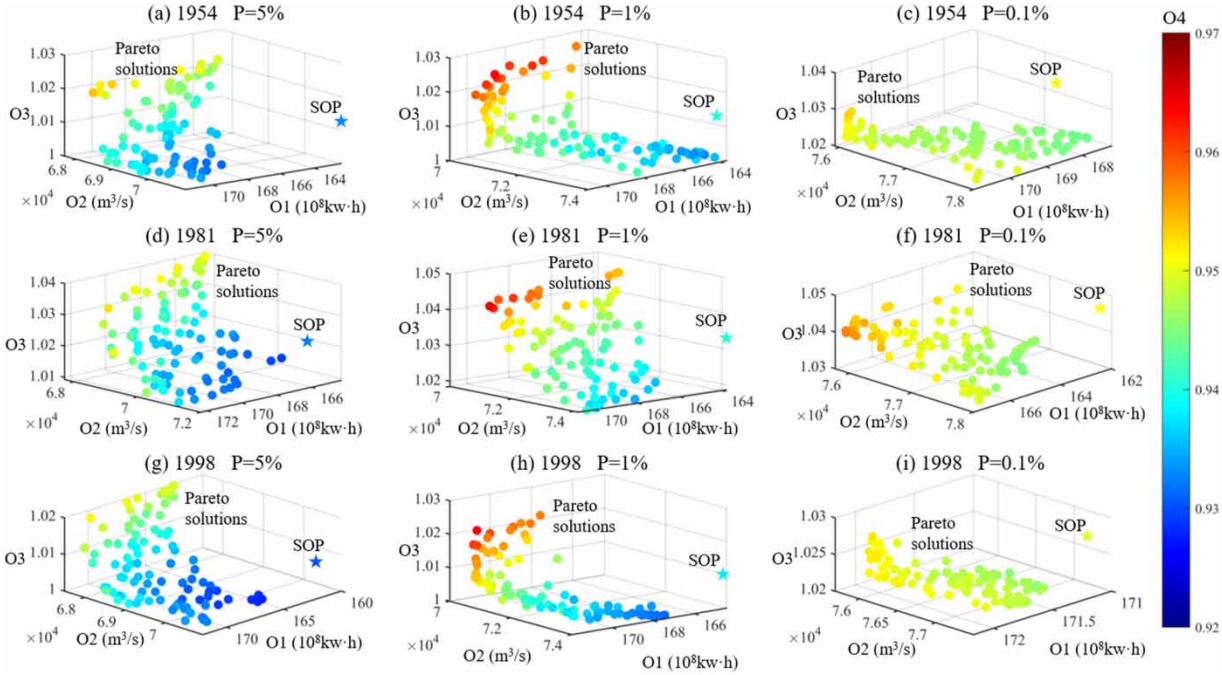

Figure 4 | Comparison of the Pareto solutions and the SOP solution in the second sub-season segment (main-flood season). O1: maximize the HG. O2: minimize the PF of the flood control station. O3: minimize the final WL of the reservoir at the flood prevention period. O4: minimize the HWL.

4.2. Multi-criteria decision-making analysis for identifying the best solution for seasonal FLWLs by the TOPSIS

The TOPSIS was utilized to determine the best operation scheme from the Pareto solutions for identifying seasonal FLWLs comprehensively considering multi-criteria of the HG, PF, WL, HWL and URS indicators. The decision-making analysis results are summarized in Table 3.

In comparison to the annual FLWLs (Table 1), for the first sub-season segment (pre-flood season), the minimal and maximal increasing values of the seasonal FLWLs for the seven mixed reservoirs are 6.51 and 9.53 m (TGR), 2.79 and 5.30 m (JY), 3.00 and 5.60 m (ZS), 0.93 and 1.65 m (DJ), 1.92 and 3.34 m (FT), 1.57 and 3.74 m (WQX), and 1.39 and 2.46 m (ZX). For the second sub-season segment (main-flood season), the minimal and maximal increasing values of the seasonal FLWLs for the seven mixed reservoirs are 1.53 and 4.18 m (TGR), 0.55 and 3.00 m (JY), 0.35 and 2.21 m (ZS), 0.13 and 0.85 m (DJ), 0.29 and 1.86 m (FT), 0.62 and 1.70 m (WQX), and 0.53 and 1.88 m (ZX). For the third sub-season segment (post-flood season), the minimal and maximal increasing values of the seasonal FLWLs for the seven mixed reservoirs are 4.36 and 8.24 m (TGR), 2.97 and 6.87 m (JY), 2.46 and 5.93 m (ZS), 0.76 and 1.65 m (DJ), 1.64 and 2.66 m (FT), 1.69 and 4.77 m (WQX), and 1.55 and 2.56 m (ZX). It is easy to find that the increments of seasonal FLWLs in the first and third sub-season segments are significantly higher than the increment of seasonal FLWLs in the third sub-season segment. That is to say, the first and third sub-season segments have more tremendous potential for developing flood resources without increasing the flood risk compared with the second sub-season segment.

For the same sub-season segment, in general, as the magnitude of design floods increases, the increment in seasonal FLWL decreases. Take the first sub-season segment (pre-flood season) for example, with respect to the design flood corresponding to the 1956 representative flood event, the seasonal FLWL of the TGR has declined from 154.26 to 151.51 m with the increase of return period from 20 to 1,000 years. The minimal (maximal) seasonal FLWL of the TGR in the second sub-season segment is 146.53 m (149.18 m), while for the first sub-season segment (the third one), the minimal and maximal seasonal FLWLs of the TGR are 151.51 and 154.53 m (149.36 and 153.24 m), respectively. From the perspectives of the three sub-season segments, because the magnitude of the design floods in the second sub-season segment is larger than that of the other two segments, the increment in seasonal FLWL of the second sub-season segment is getting smaller accordingly.

Table 3 | The best solutions obtained from the TOPSIS for seasonal FLWLs' management in the first, second and third sub-season segments

Flood season	Design flood based on	Return period (years)	TGR (m)	JY (m)	ZS (m)	DJ (m)	FT (m)	WQX (m)	ZX (m)	Score
First segment (pre-flood)	1956	20	154.26	215.28	129.08	285.47	200.96	100.98	163.51	0.661
		100	152.79	213.61	130.60	285.15	200.89	100.50	163.58	0.677
		1,000	151.51	214.10	129.05	284.93	199.92	100.86	163.43	0.642
	2007	20	154.53	215.90	130.22	285.65	201.34	101.56	164.46	0.659
		100	152.64	214.78	129.17	285.16	200.47	101.74	163.80	0.674
		1,000	151.88	213.39	128.00	285.11	200.79	99.57	163.39	0.741
Second segment (main-flood)	1954	20	148.89	211.77	127.21	284.49	199.38	99.54	162.68	0.813
		100	147.75	212.08	125.73	284.59	200.32	98.63	163.67	0.644
		1,000	146.53	211.45	125.78	284.43	199.36	98.62	162.65	0.622
	1981	20	148.18	213.60	125.83	284.55	198.91	99.70	162.53	0.734
		100	147.90	212.34	126.66	284.85	200.36	99.63	163.88	0.759
		1,000	146.71	211.15	125.35	284.59	198.79	98.97	162.85	0.661
	1998	20	149.18	212.86	126.26	284.54	199.78	98.87	163.77	0.780
		100	147.09	211.78	125.36	284.13	199.19	98.69	162.96	0.647
		1,000	146.53	211.57	126.10	284.45	199.58	99.06	162.71	0.584
Third segment (post-flood)	1952	20	153.24	214.43	130.93	285.53	201.06	102.11	164.56	0.661
		100	149.94	215.53	130.33	285.15	200.74	100.86	163.55	0.589
		1,000	149.36	215.07	127.46	285.00	200.39	100.71	163.65	0.645
	1964	20	150.25	217.47	130.39	285.65	201.16	102.77	163.62	0.723
		100	149.82	214.48	129.87	285.15	200.38	100.66	163.97	0.683
		1,000	149.76	213.57	127.81	284.76	200.14	99.69	163.65	0.695

4.3. Comparison of the best solution and the SOP solution on reservoir operation

Comparison results of the best solutions acquired from the TOPSIS and the SOP solution on the five evaluation indicators in the three sub-season segments are displayed in Figures A4, 5(a -i) and A5, respectively.

The results reveal that there are large improvements in the five evaluation indicators of the best solution with the increase of the design flood magnitude. For the first and third sub-season segments, the HG, PF and HWL indicators can be simultaneously optimized by the best solutions. The best solutions obtained from the TOPSIS, without lowering the flood prevention standard, promote the joint operation of mixed reservoir to produce 620–1,253 million kW h (4.2–10.3% improvement), 80–872 million kW h (0.5–5.4% improvement) and 171–479 million kW h (2.0–5.9% improvement) in hydropower output corresponding to the first sub-season segment (30-day flood events), the second sub-season segment (30-day flood events) and the third sub-season segment (15-day flood events). Considering the CO_2 emission reduction (0.785 kg CO_2e/kW h) related to HG over fossil energy (Zhou *et al.* 2018), the best solutions would at least decrease 487 (=620 million kW h × 0.785 kg CO_2e/kW h), 63 and 134 million kg in CO_2 emissions correspondingly. For the whole flood season, the average hydropower production of the mixed reservoir can reach 290–868 million kW h (2.9–5.1% improvement) meanwhile reducing 228–681 million kW h of the CO_2 emissions. For several main design floods, the HWL (e.g., design flood based on 1954 and 1981 with 1,000-year return periods) and the URS (e.g., design floods based on 1954) values can also be reduced in comparison to those of the SOP solution. The maximal URS value corresponding to the best solution is 217.53×10^8 m^3 (in Figure 5(f)), which is slightly less than the total flood control capacity of the mixed reservoirs (271.16×10^8 m^3, Table 1). In other words, the best solution can still reserve a partial flood storage capacity for the flood prevention safety.

The improvement rates of the five evaluation indicators obtained from the best solutions over those of the SOP solution are listed in Table 4. For all the design floods, it is found that the HG, PF and HWL indicators of the best solutions are better than those of the SOP solution with the minimal and maximal improvement rates of 0.47 and 10.26%, −4.42 and −0.06%, and −1.41 and −0.42%, respectively. This indicates that the seasonal FLWL scheme of the best solutions can improve the HG of reservoirs without increasing the flood control risk. For the first and third sub-season segments, the HWL of the best solutions is larger than that of the SOP solution because of the higher seasonal FLWLs. In addition, the URS of the best solutions is larger than that of the SOP solution for most design floods.

In summary, compared with the annual FLWL scheme (i.e., the SOP solution), the proposed seasonal FLWL schemes (i.e., the best solutions), without lowering the flood prevention standard, enhance the joint operation of mixed reservoirs to

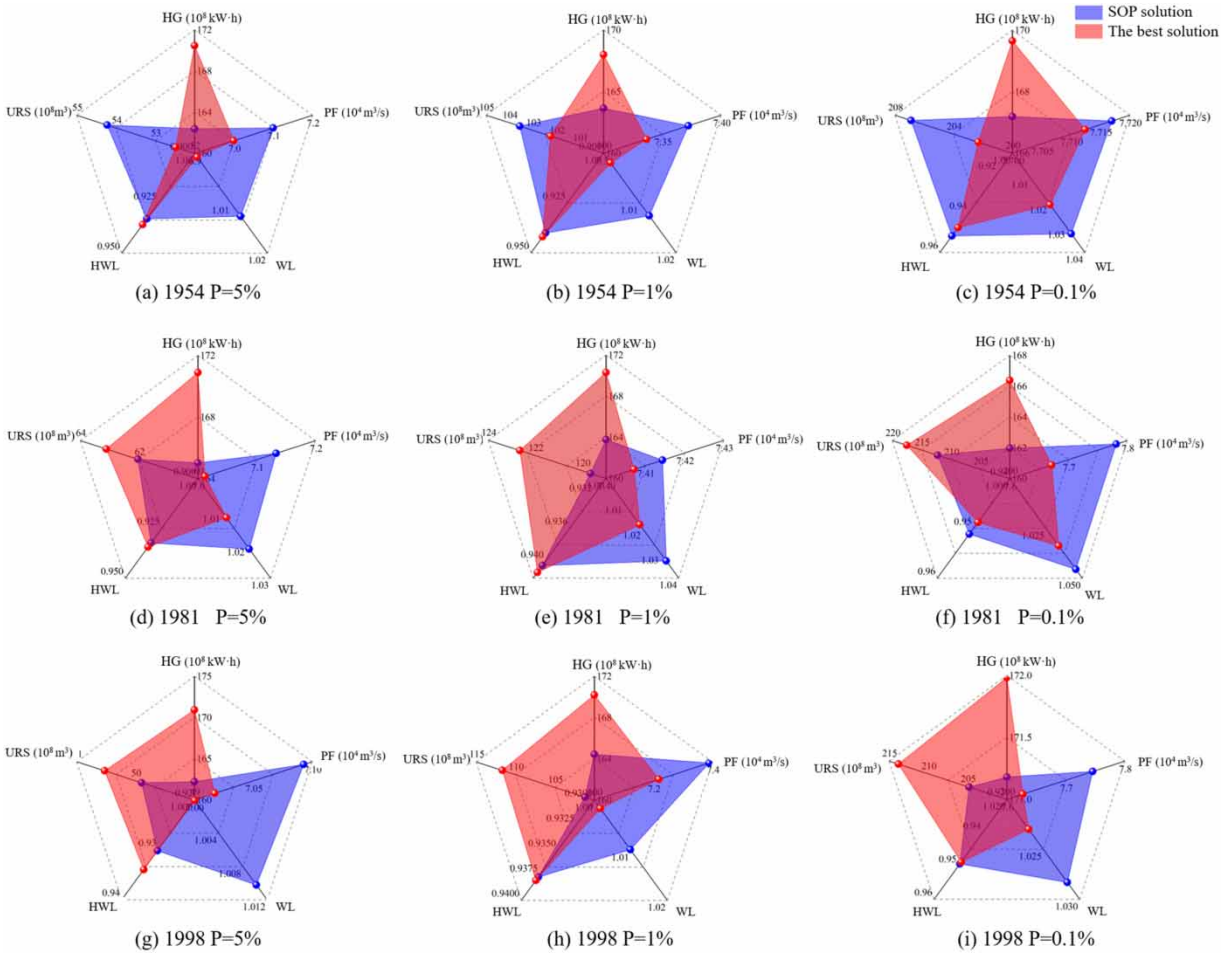

Figure 5 | Comparison of the best solution of seasonal FLWLs and the SOP solution of annual FLWL on reservoir operation for the three representative flood events in the second sub-season segment (main-flood season).

accomplish at least 620 million kW h (4.2% improvement), 80 million kW h (0.5% improvement) and 171 million kW h (2.0% improvement) in hydropower production corresponding to the first, second and third sub-season segments, meanwhile bringing down 487, 63 and 134 million kg in CO_2 emissions accordingly.

5. CONCLUSIONS

The seasonal FLWL is a crucial parameter that is used to guide reservoir operation to counterbalance the hydroelectricity production and flood prevention in different sub-season segments. The novelty of this study was to develop a multi-objective operation model of seasonal FLWLs which fused the SOP-based simulation into the NSGA-II, which was first applied to produce the Pareto solutions for trading off the demands from HG and flood prevention in seven reservoirs in the Yangtze River. Based on plenty of Pareto solutions generated from the proposed simulation–optimization framework, the TOPSIS was utilized to aptly identify the best one for seasonal FLWL management. The main conclusions are drawn below.

(1) Compared with the SOP solution, the Pareto solutions could efficiently make a tradeoff among the maximization of the hydroelectricity output (O1), the minimization of the PF of the flood control station (O2), the minimization of the final WL of the reservoir at the flood prevention period (O3) and the minimization of the HWL (O4), to skillfully cope with small–medium, large and extra-large flood events.

(2) In comparison to the annual FLWL scheme (i.e., the SOP solution) of the seven reservoirs, the best solution obtained from the TOPSIS could increase the FLWL values of the seven reservoirs from 1.39 up to 6.51 m in the first sub-

Table 4 | The improvement rates[a] of the five evaluation indicators obtained from the best solutions over those of the SOP solution in the three sub-season segments

Sub-season	Flood event	Return period (years)	Improvement rate (%)				
			HG	PF	WL	HWL	URS
Pre-flood	1956	20	9.53	−4.42	−0.65	2.02	20.45
		100	8.11	−3.15	−0.72	1.76	19.59
		1,000	4.15	−1.34	−0.60	1.40	3.03
	2007	20	10.26	−3.35	−0.80	2.51	37.09
		100	7.32	−2.84	−0.78	1.82	10.95
		1,000	4.29	−0.47	−0.79	0.92	0.74
Main-flood	1954	20	4.97	−1.41	−1.17	0.31	−3.22
		100	2.65	−0.48	−1.05	0.20	−1.26
		1,000	1.47	−0.06	−1.13	−0.44	−2.22
	1981	20	3.56	−1.70	−0.92	0.22	1.73
		100	3.98	−0.10	−1.41	0.09	2.51
		1,000	2.72	−1.41	−1.13	−0.25	2.47
	1998	20	5.38	−1.06	−1.00	0.41	1.26
		100	3.49	−2.30	−0.81	0.04	10.39
		1,000	0.47	−1.53	−0.52	−0.06	4.40
Post-flood	1952	20	5.63	−3.90	−0.81	2.21	19.56
		100	2.44	−3.06	−0.42	1.68	25.21
		1,000	2.02	−0.48	−0.91	1.02	2.16
	1964	20	5.92	−2.82	−0.84	2.00	9.88
		100	2.21	−0.85	−0.77	1.36	5.77
		1,000	2.29	−0.61	−1.02	0.69	4.74

[a]$\text{Improvement rate (\%)} = \frac{\text{Indicator\{the best solution\}} - \text{Indicator\{the SOP solution\}}}{\text{Indicator\{the SOP solution\}}} \times 100\%$.

season segment, from 0.13 up to 1.53 m in the second sub-season segment and from 0.76 up to 4.36 m in the third sub-season segment, without increasing the flood prevention risk.

(3) The proposed seasonal FLWL schemes not only could boost the reservoir operation to attain 868 million kW h/year (5.1% improvement) in average hydroelectricity output but also could decrease 681 million kg in CO_2 emissions during the flood season.

It is worth noting that the developed multi-objective optimization operation model of seasonal FLWLs in this study is aimed at efficiently counterbalancing hydropower production and flood prevention operation, meanwhile reducing CO_2 emissions associated with the use of fossil energy.

In the future, it will be interesting to conduct the research on the flood pre-discharge operation of reservoirs by integrating accurate and reliable flood forecasting information to validate the feasibility and transferability of the proposed methods.

ACKNOWLEDGEMENTS

This work was partially funded by the National Key Research and Development Program of China (2021YFC3200303) and the Research Council of Norway (FRINATEK Project 274310, KLIMAFORSK Project 302457). The authors would like to thank the editors and anonymous reviewers for their valuable and constructive comments related to this manuscript.

AUTHOR CONTRIBUTIONS

YH contributed to data curation, writing of the original draft preparation, software, and visualization. SG contributed to the conceptualization, methodology, writing of the original draft preparation, and supervision. YZ contributed to the conceptualization, methodology, reviewing and editing the writing, and supervision. DZ contributed to data curation, software, visualization, investigation, and validation. HC contributed to reviewing and editing the writing, visualization, and investigation. LX contributed to reviewing and editing the writing, investigation, and validation. JL contributed to data curation, visualization, and investigation. C-YX contributed to reviewing and editing the writing, investigation, and validation.

DATA AVAILABILITY STATEMENT

Data cannot be made publicly available; readers should contact the corresponding author for details.

CONFLICT OF INTEREST

The authors declare there is no conflict.

REFERENCES

Berga, L. 2016 The role of hydropower in climate change mitigation and adaptation: A review. *Engineering* **2** (3), 313–318. https://doi.org/10.1016/J.ENG.2016.03.004.

Chen, F., Zhou, J., Wang, C., Li, C. & Lu, P. 2017 A modified gravitational search algorithm based on a non-dominated sorting genetic approach for hydro-thermal-wind economic emission dispatching. *Energy* **121**, 276–291. https://doi.org/10.1016/j.energy.2017.01.010.

Deb, K., Agrawal, S., Pratap, A. & Meyarivan, T. 2000 A fast elitist non-dominated sorting genetic algorithm for multi-objective optimization: NSGA-II. In: *Parallel Problem Solving From Nature PPSN VI*. (Schoenauer, M., Deb, K. & Rudolph, G., eds.) Springer, Berlin, pp. 849–858.

Dhakal, N., Jain, S., Gray, A., Dandy, M. & Stancioff, E. 2015 Nonstationarity in seasonality of extreme precipitation: A nonparametric circular statistical approach and its application. *Water Resources Research* **51** (6), 4499–4515. https://doi.org/10.1002/2014WR016399.

Fang, C., Guo, S., Duan, Y. & Duong, D. 2010 Two new approaches to dividing flood sub-seasons in flood season using the fractal theory. *Chinese Science Bulletin* **55** (1), 105–110. https://doi.org/10.1007/s11434-009-0315-z.

Gao, Y., Xie, Y. H. & Zou, D. S. 2017 Using ANNs to analyse effects of the Three Gorges Dam on sedimentation in Dongting Lake, China. *Hydrological Sciences Journal* **62** (10), 1583–1590. https://doi.org/10.1080/02626667.2017.1338833.

Giuliani, M., Lamontagne, J. R., Reed, P. M. & Castelletti, A. 2021 A state-of-the-art review of optimal reservoir control for managing conflicting demands in a changing world. *Water Resources Research* **57** (12), e2021WR029927. https://doi.org/10.1029/2021WR029927.

Gonzalez, J. M., Tomlinson, J. E., Harou, J. J., Ceseña, E. A. M., Panteli, M., Bottacin-Busolin, A. & Ya, A. Z. 2020 Spatial and sectoral benefit distribution in water-energy system design. *Applied Energy* **269**, 114794. https://doi.org/10.1016/j.apenergy.2020.114794.

Hatamkhani, A., Moridi, A. & Yazdi, J. 2020 A simulation–optimization models for multi-reservoir hydropower systems design at watershed scale. *Renewable Energy* **149**, 253–263. https://doi.org/10.1016/j.renene.2019.12.055.

He, S., Guo, S., Yin, J., Liao, Z., Li, H. & Liu, Z. 2022 A novel impoundment framework for a mega reservoir system in the upper Yangtze River basin. *Applied Energy* **305**, 117792. https://doi.org/10.1016/j.apenergy.2021.117792.

Jiang, H., Wang, Z., Ye, A., Liu, K., Wang, X. & Wang, L. 2019 Hydrological characteristic-based methodology for dividing flood seasons: An empirical analysis from China. *Environmental Earth Sciences* **78** (14), 1–9. https://doi.org/10.1007/s12665-019-8392-z.

Kim, D. H., Lee, T., Shin, H. J. & Lee, S. O. 2022 Generating more hydroelecticity while ensuring the safety: Resilience assessment study for Bukhangang Watershed in South Korea. *Applied Sciences* **12** (9), 4583. https://doi.org/10.3390/app12094583.

Kuriqi, A., Pinheiro, A. N., Sordo-Ward, A. & Garrote, L. 2019 Influence of hydrologically based environmental flow methods on flow alteration and energy production in a run-of-river hydropower plant. *Journal of Cleaner Production* **232**, 1028–1042. https://doi.org/10.1016/j.jclepro.2019.05.358.

Li, X., Guo, S., Liu, P. & Chen, G. 2010 Dynamic control of flood limited water level for reservoir operation by considering inflow uncertainty. *Journal of Hydrology* **391** (1–2), 124–132. https://doi.org/10.1016/j.jhydrol.2010.07.011.

Li, C., Zhou, J., Ouyang, S., Ding, X. & Chen, L. 2014 Improved decomposition–coordination and discrete differential dynamic programming for optimization of large-scale hydropower system. *Energy Conversion and Management* **84**, 363–373. https://doi.org/10.1016/j.enconman.2014.04.065.

Liu, P., Guo, S., Xiong, L. & Chen, L. 2010 Flood season segmentation based on the probability change-point analysis technique. *Hydrological Sciences Journal* **55** (4), 540–554. https://doi.org/10.1080/02626667.2010.481087.

Liu, D., Li, X., Guo, S., Rosbjerg, D. & Chen, H. 2015a Using a Bayesian probabilistic forecasting model to analyze the uncertainty in real-time dynamic control of the flood limiting water level for reservoir operation. *Journal of Hydrologic Engineering* **20** (2), 04014036. https://doi.org/10.1061/(ASCE)WR.1943-5452.0000482.

Liu, P., Li, L., Guo, S., Xiong, L., Zhang, W., Zhang, J. & Xu, C. Y. 2015b Optimal design of seasonal flood limited water levels and its application for the Three Gorges Reservoir. *Journal of Hydrology* **527**, 1045–1053. https://doi.org/10.1016/j.jhydrol.2015.05.055.

Liu, X., Xiao, S., Pan, H., Zheng, X., Han, W., Huang, C. & Deng, S. 2022 Optimizing hydropower plants based on carbon-water-energy-ecosystem nexus. *Energy Conversion and Management* **270**, 116191. https://doi.org/10.1016/j.enconman.2022.116191.

Ma, C., Xu, R., He, W. & Xia, J. 2020 Determining the limiting water level of early flood season by combining multiobjective optimization scheduling and copula joint distribution function: A case study of three gorges reservoir. *Science of The Total Environment* **737**, 139789. https://doi.org/10.1016/j.scitotenv.2020.139789.

Mu, Z., Ai, X., Ding, J., Huang, K., Chen, S., Guo, J. & Dong, Z. 2022 Risk analysis of dynamic water level setting of reservoir in flood season based on multi-index. *Water Resources Management* 1–20. https://doi.org/10.1007/s11269-022-03188-z.

Sánchez-Lozano, J. M., García-Cascales, M. S. & Lamata, M. T. 2016 GIS-based onshore wind farm site selection using fuzzy multi-criteria decision making methods. Evaluating the case of Southeastern Spain. *Applied Energy* **171**, 86–102. http://dx.doi.org/10.1016/j.apenergy.2016.03.030.

Singh, V. P. 2011 Hydrologic synthesis using entropy theory. *Journal of Hydrologic Engineering* **16** (5), 421–433. https://doi.org/10.1061/(ASCE)HE.1943-5584.000033.

Singh, V. P., Wang, S. X. & Zhang, L. 2005 Frequency analysis of nonidentically distributed hydrologic flood data. *Journal of Hydrology* **307** (1–4), 175–195. https://doi.org/10.1016/j.jhydrol.2004.10.029.

Spanoudaki, K., Dimitriadis, P., Varouchakis, E. A. & Perez, G. A. C. 2022 Estimation of hydropower potential using Bayesian and stochastic approaches for streamflow simulation and accounting for the intermediate storage retention. *Energies* **15** (4), 1413. https://doi.org/10.3390/en15041413.

Sun, Z., Huang, Q. & Lotz, T. 2020 Evolution of flood regulation capacity for a large shallow retention lake: Characterization, mechanism, and impacts. *Water* **12** (10), 2853. https://doi.org/10.3390/w12102853.

Tamimi, V., Wu, J., Naeeni, S. T. O. & Shahvaghar-Asl, S. 2021 Effects of dissimilar wakes on energy harvesting of flow induced vibration (FIV) based converters with circular oscillator. *Applied Energy* **281**, 116092. https://doi.org/10.1016/j.apenergy.2020.116092.

Tamm, O. & Tamm, T. 2020 Verification of a robust method for sizing and siting the small hydropower run-of-river plant potential by using GIS. *Renewable Energy* **155**, 153–159. https://doi.org/10.1016/j.renene.2020.03.062.

Wan, X., Xue, Y., Hua, L. & Wu, Q. 2023 Multi-objective collaborative decision-making for flood resource utilization in a reservoir. *Stochastic Environmental Research and Risk Assessment* 1–12. https://doi.org/10.1007/s00477-023-02530-0.

Wegner, N., Mercante, E., de Souza Mendes, I., Ganascini, D., Correa, M. M., Maggi, M. F., Vilas Boas, M. A., Wrublack, S. C. & Siqueira, J. A. C. 2020 Hydro energy potential considering environmental variables and water availability in Paraná Hydrographic Basin 3. *Journal of Hydrology* **580**, 124183. https://doi.org/10.1016/j.jhydrol.2019.124183.

Xiao, Y., Guo, S., Liu, P., Yan, B. & Chen, L. 2009 Design flood hydrograph based on multicharacteristic synthesis index method. *Journal of Hydrologic Engineering* **14** (12), 1359–1364. 4. https://doi.org/10.1061/(ASCE)1084-0699(2009)14:12(1359).

Xie, A., Liu, P., Guo, S., Zhang, X., Jiang, H. & Yang, G. 2018 Optimal design of seasonal flood limited water levels by jointing operation of the reservoir and floodplains. *Water Resources Management* **32** (1), 179–193. https://doi.org/10.1007/s11269-017-1802-7.

Xiong, F., Guo, S., Yin, J., Tian, J. & Rizwan, M. 2020 Comparative study of flood regional composition methods for design flood estimation in cascade reservoir system. *Journal of Hydrology* **590**, 125530. https://doi.org/10.1016/j.jhydrol.2020.125530.

Yazdi, J. & Moridi, A. 2018 Multi-objective differential evolution for design of cascade hydropower reservoir systems. *Water Resources Management* **32** (14), 4779–4791. https://doi.org/10.1007/s11269-018-2083-5.

Yun, R. & Singh, V. P. 2008 Multiple duration limited water level and dynamic limited water level for flood control, with implications on water supply. *Journal of Hydrology* **354** (1–4), 160–170. https://doi.org/10.1016/j.jhydrol.2008.03.003.

Zhang, H., Chang, J., Gao, C., Wu, H., Wang, Y., Lei, K. & Zhang, L. 2019 Cascade hydropower plants operation considering comprehensive ecological water demands. *Energy Conversion and Management* **180**, 119–133. https://doi.org/10.1016/j.enconman.2018.10.072.

Zheng, T., Qiang, M., Chen, W., Xia, B. & Wang, J. 2016 An externality evaluation model for hydropower projects: A case study of the Three Gorges Project. *Energy* **108**, 74–85. https://doi.org/10.1016/j.energy.2015.10.116.

Zhou, Y., Guo, S., Liu, P. & Xu, C. 2014 Joint operation and dynamic control of flood limiting water levels for mixed cascade reservoir systems. *Journal of Hydrology* **519**, 248–257. https://doi.org/10.1016/j.jhydrol.2014.07.029.

Zhou, Y., Guo, S., Xu, J., Zhao, X. & Zhai, L. 2015 Risk analysis for seasonal flood-limited water level under uncertainties. *Journal of Hydro-Environment Research* **9** (4), 569–581. https://doi.org/10.1016/j.jher.2015.05.001.

Zhou, Y., Guo, S., Chang, F. J., Liu, P. & Chen, A. B. 2018 Methodology that improves water utilization and hydropower generation without increasing flood risk in mega cascade reservoirs. *Energy* **143**, 785–796. https://doi.org/10.1016/j.energy.2017.11.035.

Zhou, Y., Chang, L. C., Uen, T. S., Guo, S., Xu, C. Y. & Chang, F. J. 2019 Prospect for small-hydropower installation settled upon optimal water allocation: an action to stimulate synergies of water-food-energy nexus. *Applied Energy* **238**, 668–682. https://doi.org/10.1016/j.apenergy.2019.01.069.

Zhou, Y., Chang, F. J., Chang, L. C., Lee, W. D., Huang, A., Xu, C. Y. & Guo, S. 2020 An advanced complementary scheme of floating photovoltaic and hydropower generation flourishing water-food-energy nexus synergies. *Applied Energy* **275**, 115389. https://doi.org/10.1016/j.apenergy.2020.115389.

Zhu, D., Chen, H., Mei, Y., Xu, X. & Guo, S. 2022a Exploration of relationships between flood control capacity and peak flow reduction in a multireservoir system using an optimization-clustering-fitting framework. *Journal of Water Resources Planning and Management* **148** (5), 05022002. https://doi.org/10.1061/(ASCE)WR.1943-5452.0001549.

Zhu, D., Chen, H., Zhou, Y., Mei, Y., Xu, X. & Guo, S. 2022b A triple-stage operation method for deriving operation rules for cascade reservoirs during catastrophic flood events. *Water Resources Management* 1–21. https://doi.org/10.1007/s11269-022-03189-y.

Zhu, D., Chen, H., Zhou, Y., Xu, X., Guo, S., Chang, F. J. & Xu, C. Y. 2022c Exploring a multi-objective cluster-decomposition framework for optimizing flood control operation rules of cascade reservoirs in a river basin. *Journal of Hydrology* **614**, 128602. https://doi.org/10.1016/j.jhydrol.2022.128602.

First received 19 May 2023; accepted in revised form 8 December 2023. Available online 22 January 2024